BOND-GRAPH BASED CONTROLLER DESIGN OF A TWO-INPUT TWO-OUTPUT FOUR-TANK SYSTEM

Nacusse, Matías A.[(a)] and Junco, Sergio J.[(b)]

LAC, Laboratorio de Automatización y Control, Departamento de Control, Facultad de Ciencias Exactas, Ingeniería y Agrimensura, Universidad Nacional de Rosario, Ríobamba 245 Bis – S2000EKE Rosario – Argentina.

[(a)]nacusse@fceia.unr.edu.ar, [(b)]sjunco@fceia.unr.edu.ar

ABSTRACT

The quadruple-tank process has been proposed as a benchmark for multivariable control system design. This paper addresses the design in the bond graph domain of a robust controller having the volumetric flows of two pumps as manipulated variables and the level of the two lower tanks as the regulated outputs. The basic control objectives, expressed in terms of desired closed-loop energy and power-dissipation functions, are captured in the bond graph domain means a so-called Target Bond Graph, and the controller design is performed via Bond-Graph prototyping. The basic control law is further robustified against parameter uncertainties, measurement deviations and faults using the diagnostic bond graph concept, what leads to an additional loop consisting in a PI-law also being expressed with a physically meaningful bond graph subsystem. Some causal manipulations on the four-tank bond graph allow to extend to this multi-variable case the technique developed to solve the simpler monovariable two-tank control problem.

Keywords: quadruple-tank system, bond graph prototyping, robust fault-tolerant control, non-linear energy-based control.

1. INTRODUCTION

The quadruple-tank system proposed in (Johansson 2000) turned into a very popular benchmark allowing to test different control algorithms for multivariable processes. It is a Two-Input Two-Output or TITO nonlinear plant consisting of four interconnected water tanks fed by two pumps, whose linearized model has a multivariable zero, which can be made minimum or non-minimum phase by simply changing the position of two distribution valves. This system has been used to test and design several control schemes. In (Abdullah and Zribi 2012) a bibliographical review and three different control schemes are presented; gain scheduling, a linear parameter varying controller and input-output feedback linearization have been compared, measuring the pressure of the four tanks. In (Johnsen and Allgöwer 2007) an interconnection and damping assignment plus passivity based control (IDA-PBC) algorithm for the minimum phase configuration of the four-tank system is presented showing simulation and experimental results. Limon, et al. 2010 present a robust model predictive control (MPC) algorithm for level tracking. In both cases the level of the four tanks are measured.

This paper addresses the design in the Bond Graph (BG) domain of an energy-based nonlinear control law which only measures the pressures of the two bottom tanks. The control system design objectives are to track the levels (or pressures) of the two bottom tanks, to reject disturbances originated in model uncertainties and measurement errors, and to be tolerant to some interconnection faults.

Fault tolerant control (FTC) can be classified in two main categories, Passive Fault Tolerant Control (PFTC) and Active Fault Tolerant Control (AFTC). Both approaches are usually complemented in the praxis to improve the performance and stability of the fault tolerant system (Blanke, et al. 2006). Refer to (Zhang and Jiang 2008) for a bibliographical and historical review on FTC. The passive approach defines a unique control law to achieve the control objectives even in the presence of a fault. Generally speaking, the passive approach ensures stability and confers robustness under faults to the control system, but there exists a trade-off between performance and robustness (Isermann 2006). Although this paper follows a PFTC-approach, some concepts commonly found in the design of AFTC controllers are used.

The active approach modifies the control law according to the faults occurred, so that in this approach a fault detection and isolation (FDI) phase is mandatory before making a decision on how to reconfigure the control law. Analytical redundancy relationships (ARR), which count among the many solutions used to generate residual signals for FDI, have been implemented in the BG domain via the Diagnostic Bond Graphs (DBG) technique presented in (Samantaray, et al. 2006). Using the plant inputs and plant measurements, residual signal are generated that depend on the model parameters and the real plant parameters.

Nacusse and Junco (2011) address the PFTC-problem of a two-tank system in the BG domain using

an energy and power shaping method (Junco 2004). This method first expresses the control system specifications in terms of desired closed-loop energy and power dissipation functions, proceeds further capturing both functions in a so called Target Bond Graph (TBG) that represents the desired closed-loop behaviour, and concludes constructing the controller via Bond Graph prototyping. This prototyping is such that the coupling of the resulting controller-BG and the plant-BG renders the whole equivalent to the TBG. In Nacusse and Junco (2011) the basic control law obtained in this way is robustified with additional terms derived considering a Diagnostic Bond Graph (DBG) of the closed-loop: the *nominal* control system represented by the TBG (originally proposed under ideal assumptions) is fed with the actual reference signals and measured plant outputs. Thus, the residual signal obtained from the closed loop DBG (CL-DBG) is a measure of the error between the desired and the actual dynamics of the control system. So, the control law aims at making the residual signal vanish in time, making the closed-loop system to behave asymptotically like the original TBG.

The rest of the paper is organized as follows. Section 2 reviews some background results and summarizes the main results presented in Nacusse and Junco (2011). Section 3, revisiting this previous result on the two-tank system, addresses some BG manipulations that simplifies the controller and, simultaneously, provides a way to extend the design method employed in the simpler system to the multivariable four-tank process which in shown in Section 4. Next, Section 5 presents some simulation responses that prove the good dynamic response of the control system and, finally, Section 6 addresses some conclusions.

2. BACKGROUND AND PREVIOUS RESULTS

This section briefly summarizes the main ideas on performing energy shaping and damping assignment directly in the BG domain through BG prototyping and recalls their application to solve a control problem on a two-tank system as presented in Nacusse and Junco (2011). This result will be revised in the next section as a prelude to the development of the main result in this paper, the design of a controller for the quadruple-tank benchmark process.

2.1. Energy- based control in the BG domain

The power and energy shaping control technique defines the control problem as a stabilization one, choosing desired closed-loop energy- and power-dissipation functions, and obtaining the control law through equations that match the control open-loop energy function (a kind of control Lyapunov function, see Sontag 1998) and the desired closed-loop functions. Passivity-based control on port-Hamiltonian models count among the most successful (Ortega, et al., 2002, Ortega, et al., 2008).

In the BG domain, the closed-loop specifications are expressed by a so-called Target Bond Graph (TBG) representing the equivalent closed-loop behavior. In order to obtain the control law, the controlled sources – which provide the manipulated variables in the BG model of the plant– are prototyped (meaning that their behavior is expressed means BG components) in such a way that their power-interconnection with the rest of the plant BG –which is called a Virtual BG (VBG)– matches the TBG.The control law is obtained from the VBG by simply reading the outputs of the prototyped sources with the help of the causal assignment in the VBG. This method is exemplarily performed below on a two-tank system. For more details refer to (Junco 2004).

2.2. Control via BG-prototyping: the 2-tank system

As shown in Figure 1, the tanks are located one above the other, the upper tank discharging into the lower tank. Both tanks are fed with a unique input flow splitted between them through a distribution valve whose parameter $\gamma \in [0,1]$ determinates how the input flow is distributed to the tanks as indicated by the BG in Figure 1.

The control objectives imposed on *Tank1* are:

- Tracking of constant reference levels
- Rejection of constant disturbances.
- Robustness regarding parametric uncertainties and faults.

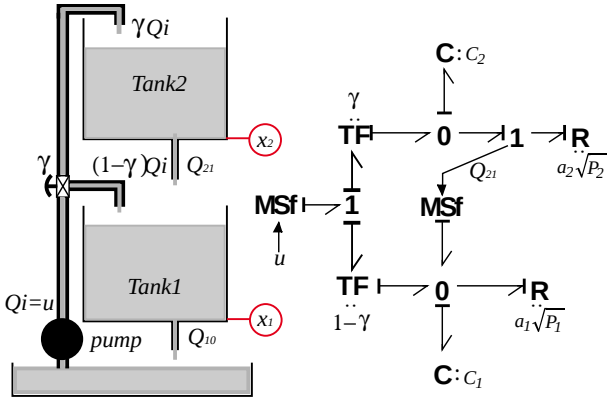

Figure 1: Two-tank system and its BG model. Measured plant outputs encircled in red.

The state equations can be read from the BG of Figure 1 using the standard procedure, giving as state variables the stored liquid volumes. Here the gauge pressures at the bottom of the tanks are chosen as state variables (instead the liquid levels used in Nacusse and Junco 2011) and presented in (1):

$$\dot{x}_1 = -\frac{a_1\sqrt{x_1}}{c_1} + \frac{a_2\sqrt{x_2}}{c_1} + \frac{(1-\gamma)}{c_1}u$$
$$\dot{x}_2 = -\frac{a_2\sqrt{x_2}}{c_2} + \frac{\gamma}{c_2}u \qquad (1)$$

Where, with $i=1,2$, x_i represents the gauge pressure at the bottom of *Tanki*; C_i are the tanks hydraulic capacities and a_i are coefficients depending on the cross sections of the outlet holes of the tanks.

The proposed TBG for the closed loop system is shown in Figure 2 where the desired stored energy and power dissipation are expressed in terms of the tracking error state variable in (2) and (3).

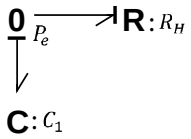

Figure 2: TBG for pressure control of lower tank.

$$V(x) = \frac{1}{2} C_1 {x_e}^2$$
$$\dot{V}(x) = -\frac{1}{R_H} {x_e}^2 \quad (2)$$

$$\dot{x}_e = -\frac{1}{C_1 R_H} x_e \quad (3)$$

The tracking error $x_e = x_1 - x_1^{ref}$ is the state variable of the TBG and x_1^{ref} is the *Tank1* reference pressure.

To enforce the desired closed-loop dynamics specified by the TGB, the Virtual BG (VBG) of Figure 3 is constructed. It shows how to proceed in order to obtain the control law. The left half of the figure is obtained prototyping the controlled power source **MSf** in such a way that access is gained to the chosen output, the pressure x_1, and an overall equivalent behavior to the TBG is achieved. The first objective is achieved via the exact compensation of the *Tank2* pressure on the pump over the distribution valve and of the discharge of *Tank2* on *Tank1*. The second objective is reached first adding the virtual elements with negative "gains" that cancel the own dynamics of *Tank1* and later building the incremental dynamics around the reference pressure P_1^{ref} for *Tank1* via the insertion of the virtual elements **C**: $C_1$and **MSe** (shapes the closed-loop energy) and **R**: R_H (damping assignment).

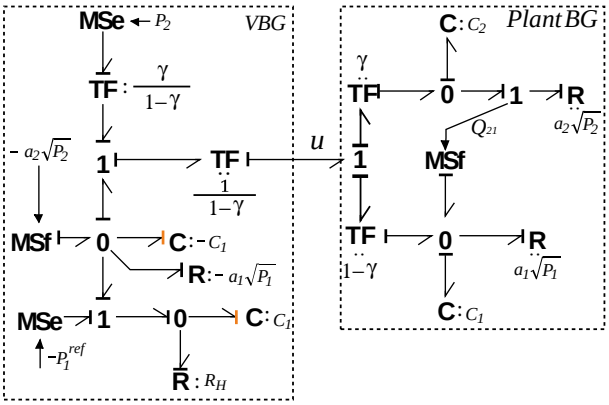

Figure 3: Virtual and plant BG.

Using the standard causality reading procedure the control law (12)can be read directly from the VBG as:

$$u = \left(\frac{1}{1-\gamma}\right)\left[a_1\sqrt{x_1} - a_2\sqrt{x_2} - \frac{1}{R_H}\left(x_1 - x_1^{ref}\right) + C_1 \dot{x}_1^{ref}\right] \quad (4)$$

Assuming exact model knowledge and perfect measurements, this control law yields a closed-loop behavior equivalent to the TBG of Figure 2, i.e., the closed-loop dynamics satisfies (3).

Remark: the rated control law (4) performs a *partial* energy shaping and damping assignment, since only the dynamics of *Tank1* is captured in the TBG. As no objectives are imposed on *Tank2* and its dynamics is hidden in closed-loop, its stability must be analyzed after the controller has been designed, property that can be easily verified in this case.

Perturbed closed-loop dynamics. Because of parameter dispersion, faults, modeling errors, sensor limited precision, noise, etc., neither the model nor the measurements are exact. To deal with this it is convenient to think the control input as composed by two terms as in (5), where u_r is the "rated" part of u, i.e., the control input part that performs the power and energy shaping under ideal plant and measurement conditions. In the same expression, δ_u is the unknown controller part due to modeling errors, parametric dispersion, faults, etc. The BG of Figure 4 reflects this situation.

$$u = u_r + \delta_u \quad (5)$$

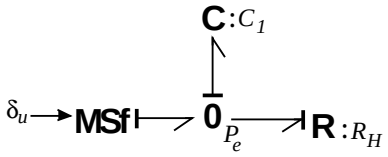

Figure 4: Perturbed TBG.

Under this situation the closed-loop dynamics no longer satisfies (3) but (6).

$$\dot{x}_e = -\frac{1}{C_1 R_H} x_e + \frac{1}{C_1}\delta_u \quad (6)$$

2.3. Robustifying the control law

The CL-DBG is defined injecting the pressure tracking error (as measured on the real control system) into the TBG through modulated sources and collecting a residual signal as shown in Figure 5.

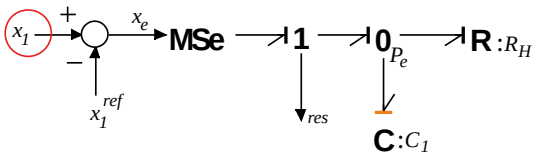

Figure 5: Proposed CL-DBG. Measurements to be fed encircled in red.

The CL-DBG yields to the new error dynamics in (7) which is driven by the residual signal res. The residual signal, which is the power co-variable of the error

injected into the CL-DBG, is a measure of the difference between the actual and the ideally expected closed-loop dynamics, i.e., when $res = 0$, x_e responds as previously defined in the TBG of Figure 2. This suggests that the control objectives could be reached extending the previously computed control law to a new one $u = u(x_1, x_2, x_1^{ref}, res)$ incorporating the residual signal in such a way that res tends to zero with growing time.

$$\dot{x}_e = -\frac{1}{C_1 R_H} x_e + \frac{res}{C_1} \quad (7)$$

The residual expression (8) obtained reading the CL-DBG clearly shows that choosing u as in (4) (rated control law) yields $res = 0$, in absence of faults and modeling errors.

$$res = -a_1\sqrt{x_1} + a_2\sqrt{x_2} + \frac{1}{R_H}\left(x_1 - x_1^{ref}\right) - C_1\dot{x}_1^{ref} + (1-\gamma)u \quad (8)$$

To improve the control system robustness, the extra term u_4 shown in (9) is added to the expression (4) for u.

$$u = \left(\frac{1}{1-\gamma}\right)\left[a_1\sqrt{x_1} - a_2\sqrt{x_2} - \frac{1}{R_H}\left(x_1 - x_1^{ref}\right) + C_1\dot{x}_1^{ref} + u_4\right] \quad (9)$$

Choosing $u_4 = -K\int res$ yields the residual dynamics (10):

$$\dot{res} + K\, res = (1-\gamma_n)\dot{\delta_u} \quad (10)$$

Thus, with constant δ_u, res goes asymptotically to zero with time constant $1/K$. As already anticipated, this forces x_e to approach asymptotically the desired error dynamics defined in the TBG of Figure 2.

Representing u_4 in terms of $\left(x_1 - x_1^{ref}\right)$ yields (11), expression showing that, in this case, the residual signal defined in the CL-DBG has a PI structure. Note however that this does not necessarily generalize, since the resulting structure depends on the TBG.

$$u_4 = -KC_1\left(x_1 - x_1^{ref}\right) - \frac{K}{R_H}\int\left(x_1 - x_1^{ref}\right) \quad (11)$$

3. THE TWO-TANK PROBLEM REVISITED

In this Section the two-tank problem is revisited. First, a causal manipulation of the original system BG is shown which leads to a simplification of the control law and will be advantageously used in the process of deriving the control law for the quadruple-tank system. Second, a BG interpretation of the robustifying additional term is provided.

3.1. Causal manipulation and simplified control law

In Figure 1 the flow Q_{21} from *Tank2* into *Tank1* is computed by the **R**-element representing the discharge orifice of the former. Putting in derivative causality the upper **C**-element (models the potential energy stored in the upper tank) yields the BG of Figure 6, where the discharging flow is computed as the sum of the incoming flow from the source and the output flow to the upper **C** element, i.e., $Q_{21} = \gamma u - Q_{c2}$. This new computation justifies the equivalent BG of Figure 7.

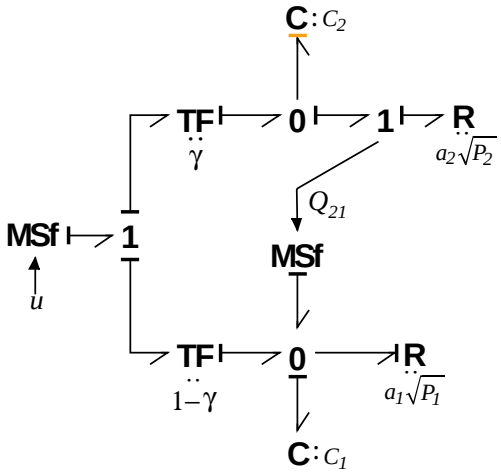

Figure 6: BG model of the two tanks system with the upper C in derivative causality.

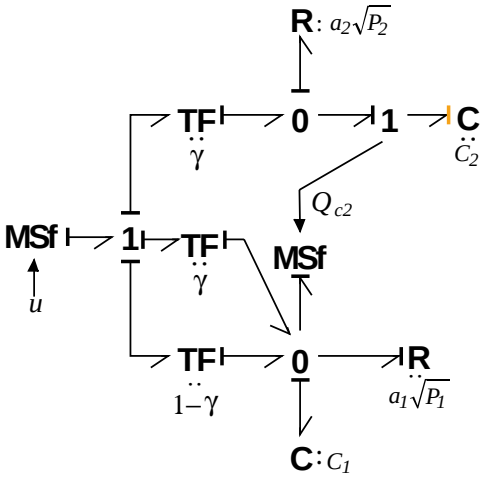

Figure 7: Equivalent plant model after manipulation of the original BG.

Furthermore, as the control objectives are placed only on *Tank1*, for control system design purposes the equivalent plant model shown in Figure 8 can be considered, where the effect of *Tank2* enters as a disturbance.

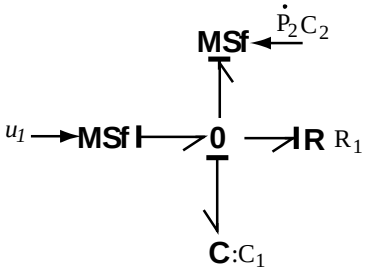

Figure 8: Equivalent control system design BG.

Following similar steps as those detailed in Section 2.2, the VBG of Figure 9 can be constructed to enforce the desired closed-loop dynamics specified by the TGB.

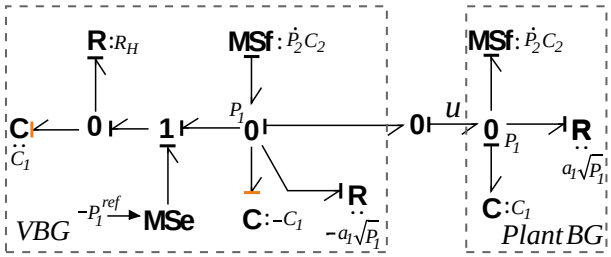

Figure 9: Virtual and plant BG.

The control law (12) can be read directly from the VBG using the standard causality reading procedure:

$$u = a_1\sqrt{x_1} - \frac{1}{R_H}\left(x_1 - x_1^{ref}\right) + C_1\dot{x}_1^{ref} + C_2\dot{x}_2 \qquad (12)$$

Remark: Equations (4) and (12) are fully equivalent and both show the need to measure not only the pressure of *Tank1* but also that of *Tank2* to implement the control law *u*. However, equation (12) – which results from the above manipulation performed on the BG– has the advantage of showing that its last term can be eliminated from the control law as it is an evanescent perturbation, i. e., it vanishes in steady state, and as such it does not affect the equilibrium point. Doing so yields the control law (13) which can be implemented with the sole measurement of x_1. However, it must be realized that this simplification amounts to modifying the TBG as indicated in Figure 10.

$$u = a_1\sqrt{x_1} - \frac{1}{R_H}\left(x_1 - x_1^{ref}\right) + C_1\dot{x}_1^{ref} \qquad (13)$$

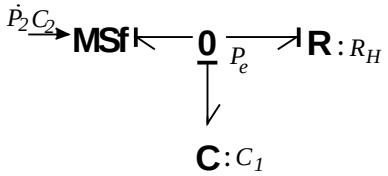

Figure 10: New TBG without measuring x_2.

3.2. BG interpretation of the robustifying term

This subsection revisits the result of (Nacusse and Junco 2011) summarized in Section 2.3 of this paper in order to provide a BG implementation of the additional term u_4 of the control law given in (11).

The TBG defines the closed loop dynamics of the system. To robustify its behavior it is necessary to inject an additional control action. In order to analyze this problem in the BG domain a concise word BG version of Figure 9 is presented in Figure 11. Departing from Figure 11, Figure 12 shows the word BG of a power interconnection proposed as a means to provide the additional control action. There, the word BG block named *mDBG* must be capable of rejecting all of the above-mentioned disturbances.

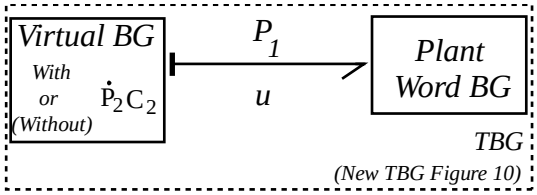

Figure 11: Power coupling between plant BG and VBG to obtain the TBG.

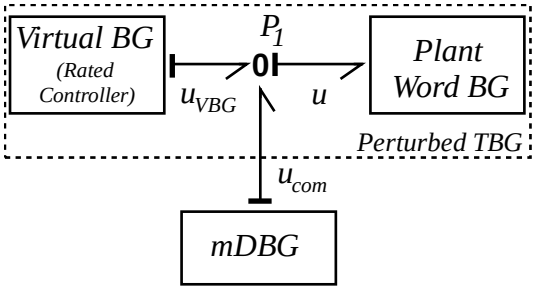

Figure 12: Proposed power interconnection

In the approach presented in Nacusse and Junco (2011) a residual signal is generated through a CL-DBG as indicated in Figure 13 (cf. Figure 5) (see Appendix B for a brief description of the DBG for FDI purposes). This residual measures the error between the PTBG and the TBG and is used to generate an additional control action forcing this error to vanish in steady-state (as well as the residual itself).

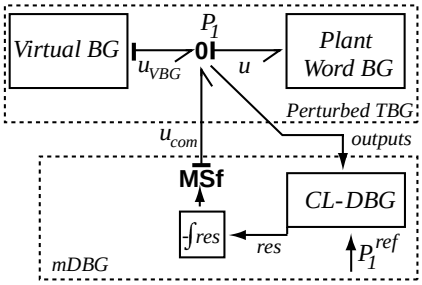

Figure 13: Signal coupling between PTBG and TBG through closed loop DBG.

The additional control action u_4 (a hydraulic flow) given in (11) in terms of the tracking error (a pressure) can be interpreted as produced by an effort-sharing set of a hydraulic resistance and inertance**,** i.e., an **I**- and a **R**-element. Figure 14 shows the resulting closed loop BG with power coupling between the PTBG and the *mDBG*, where $R_1 = 1/KC_1$ and $I_1 = R_H/K$.

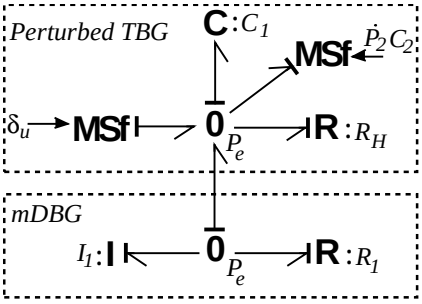

Figure 14: Power coupling between the PTBG and the mDBG.

Figure 15 shows the resulting closed loop BG, where the power interconnection among the plant BG, the VBG and the *mDBG* is highlighted in dotted squares. Notice that the redundancy in the MSe which injects the $-P_1^{ref}$ can be eliminated by shifting the *mDBG* into the VBG as it is shown in Figure 16.

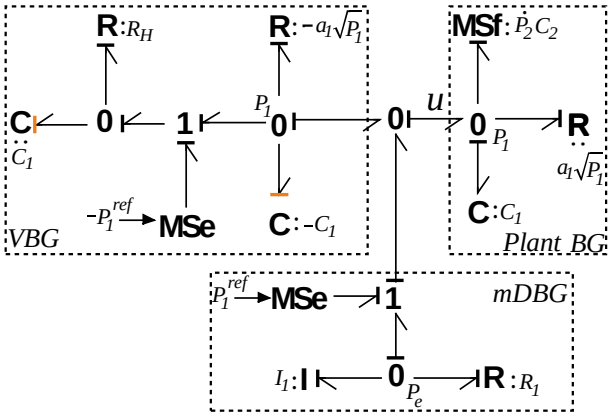

Figure 15: Resulting closed loop BG.

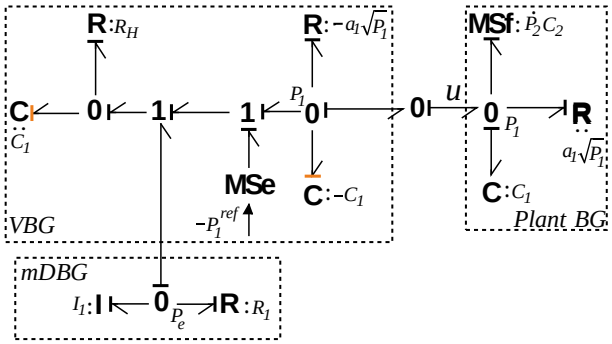

Figure 16: Closed loop BG with mDBG coupled into the VBG

Remark: As already anticipated, with constant δ_u, the tracking error x_e approaches zero asymptotically, as it can be easily verified through a causal and power analysis of the BG in Figure 14. Indeed, with constant disturbances at the outputs of both **MSf**, the **I**-element integrates its input effort P_e until it is driven to zero. At the same time, the **I**-element keeps at its output a constant flow-value which exactly cancels the sum of the **MSf**-flows and, thus, generates a zero-flow situation at the input of the **C**-element, which in turn keeps P_e in zero, which is precisely the control objective. The stability of this situation depends on the **R** elements being strictly dissipative (Junco 2001), which is of course ensured by design.

4. APPLICATION TO THE FOUR-TANK BENCHMARK PROBLEM

The four-tank system depicted in Figure 17 is a TITO nonlinear plant consisting of four interconnected water tanks fed by two pumps, whose linearized model has a multivariable zero, which can be made minimum or non-minimum phase by simply changing the position of two distribution valves.

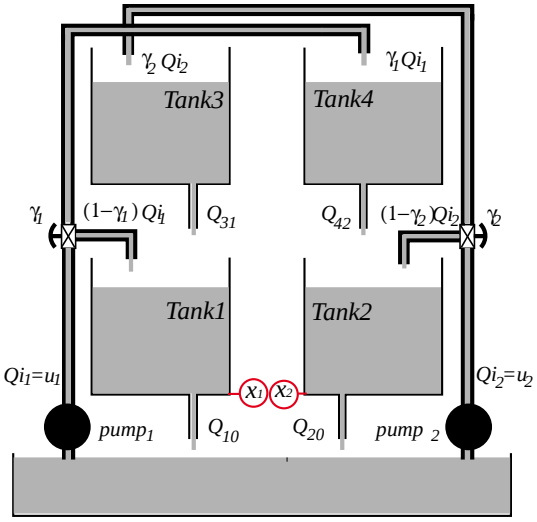

Figure 17: Four-tank system with measurements encircled in red.

4.1. Causal manipulation and controller design

In this subsection the control law for the four-tank system is designed. The control objectives are the same of that proposed for the two-tank system, in this case imposed on both of the bottom tanks.

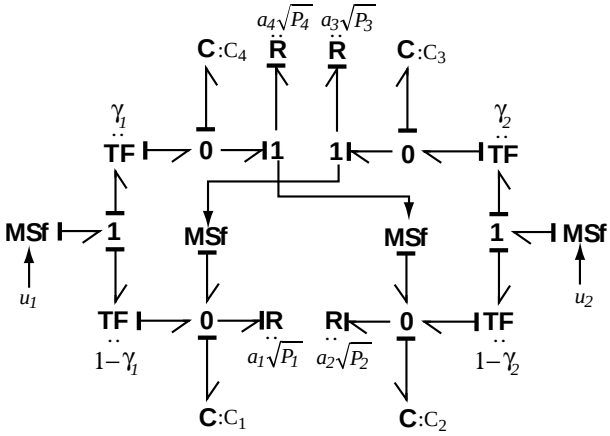

Figure 18: BG model of the four-tank system.

As the first step developing the multivariable control law, a causal manipulation is performed on the original BG of Figure 18 as shown in Figure 19. Similarly as in the two-tank case, again the discharge flows of the upper tanks are expressed not as computed by their associated **R**-elements but as the difference between the flows of the sources minus their net input flows ($\gamma_1 u_1 - C_3\dot{P}_3$ and $\gamma_2 u_2 - C_4\dot{P}_4$). This manipulation permits to construct the new BG given in Figure 20. This BG exhibits two internal variables u_1^* and u_2^*, which in the sequel are going to be treated as virtual control inputs. Seen from the bonds associated to these two auxiliary flow variables the quadruple-tank problem appears as two decoupled two-tank problems. Hence, the multivariable problem is strongly simplified, as the previously developed procedure can be first applied to each sub-problem and then the overall control law be recovered using the causal relationships relating the

auxiliary variables with the control inputs provided by the power-conserving structure.

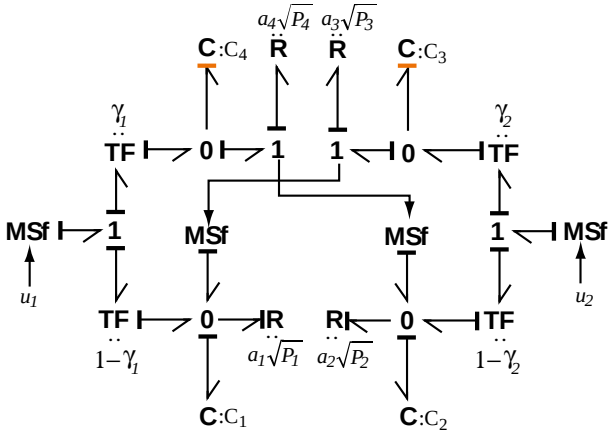

Figure 19: BG of the four tanks system with upper tanks in derivative causality.

The real and the virtual control inputs are related through a transformation matrix which is given in (14). Notice that when $\gamma_1 + \gamma_2 = 1$ the transformation matrix is singular. In this condition of the distribution valves the multivariable zeros (of the linearized system) are placed at the origin of the complex plane.

$$\begin{bmatrix} u_1^* \\ u_2^* \end{bmatrix} = \begin{bmatrix} (1-\gamma_1) & \gamma_2 \\ \gamma_1 & (1-\gamma_2) \end{bmatrix} \begin{bmatrix} u_1 \\ u_2 \end{bmatrix} \tag{14}$$

The virtual control laws, obtained following the same procedure as in the two-tank example ignoring the vanishing term, are given in (15).

$$\begin{aligned} u_1^* &= a_1\sqrt{x_1} - \frac{1}{R_{H1}}\left(x_1 - x_1^{ref}\right) + C_1\dot{x}_1^{ref} \\ u_2^* &= a_2\sqrt{x_2} - \frac{1}{R_{H2}}\left(x_2 - x_2^{ref}\right) + C_2\dot{x}_2^{ref} \end{aligned} \tag{15}$$

4.2. Robustifying the control law

The virtual control laws (15) are robustifyied, as in the two-tank example, via power coupling of the *mDBG* or by simply adding a term like (11) to each equation of (15). This yields the real control laws given in (16) and (17).

$$\begin{aligned} u_1 = -\frac{1}{\gamma_1+\gamma_2-1}\Big\{(1-\gamma_2)\Big[a_1\sqrt{x_1} - \frac{x_1-x_1^{\mathrm{ref}}}{R_{\mathrm{H1}}} + C_1\dot{x}_1^{\mathrm{ref}} - \\ K_1C_1\left(x_1 - x_1^{\mathrm{ref}}\right) - \frac{K_1}{R_{\mathrm{H1}}}\int\left(x_1 - x_1^{\mathrm{ref}}\right)\Big] - \gamma_2\Big[a_2\sqrt{x_2} - \\ \frac{x_2-x_2^{\mathrm{ref}}}{R_{\mathrm{H2}}} + C_2\dot{x}_2^{\mathrm{ref}} - K_2C_2\left(x_2 - x_2^{\mathrm{ref}}\right) - \frac{K_2}{R_{\mathrm{H2}}}\int\left(x_2 - \\ x_2^{\mathrm{ref}}\right)\Big]\Big\} \end{aligned} \tag{16}$$

$$\begin{aligned} u_2 = -\frac{1}{\gamma_1+\gamma_2-1}\Big\{(1-\gamma_1)\Big[a_2\sqrt{x_2} - \frac{x_2-x_2^{ref}}{R_{H2}} + C_2\dot{x}_2^{ref} - \\ K_2C_2\left(x_2 - x_2^{ref}\right) - \frac{K_2}{R_{H2}}\int\left(x_2 - x_2^{ref}\right)\Big] - \gamma_1\Big[a_1\sqrt{x_1} - \\ \frac{x_1-x_1^{ref}}{R_{H1}} + C_1\dot{x}_1^{ref} - K_1C_1\left(x_1 - x_1^{ref}\right) - \frac{K_1}{R_{H1}}\int\left(x_1 - \\ x_1^{ref}\right)\Big]\Big\} \end{aligned} \tag{17}$$

Using (16) and (17) the stability of the hidden closed-loop dynamics of *Tank_3* and *Tank_4* can be verified.

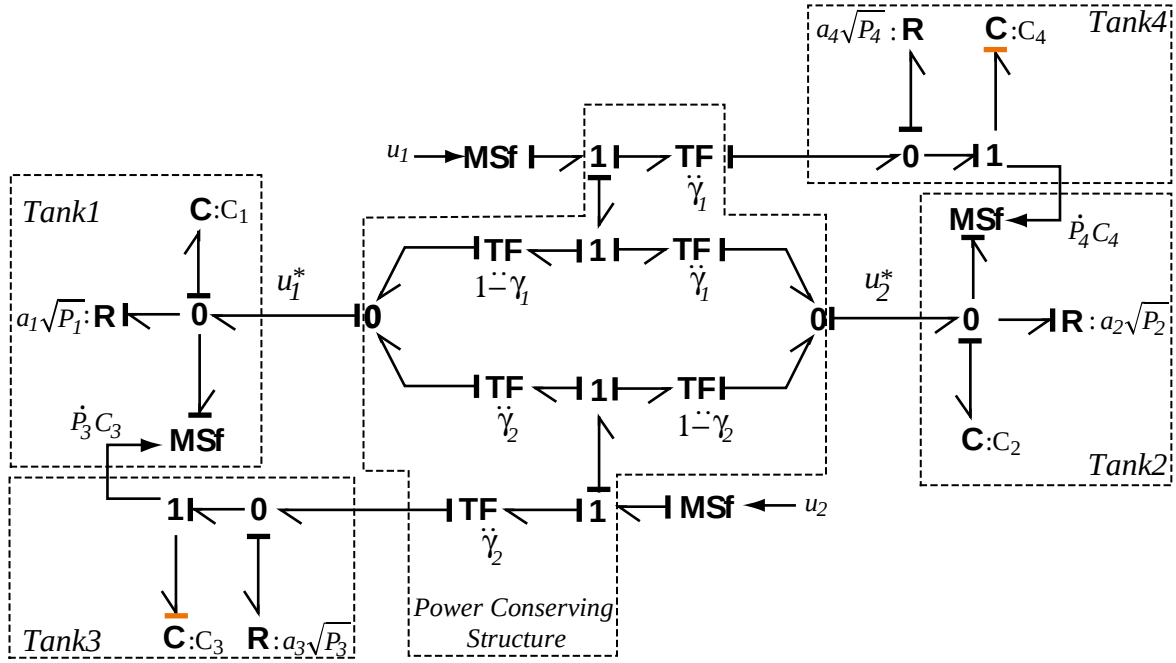

Figure 20: BG model after manipulation for controller design.

5. SIMULATION RESULTS.

The parameters used in the simulations, shown in Table I, were obtained from (Johansson 2000), where A_i are the cross section areas of the tanks, related to the tanks hydraulic capacities by the relation $C_i = A_i/\rho g$ where ρ is the liquid (water) density and g is the gravitational acceleration. The parameters of the *mDBG* are $R_{H1} = R_{H2} = 10$ and $K_1 = K_2 = 0.01$.

Table I. Simulation parameters

Parameter	Value
A_1, A_3	$28\ cm^2$
A_2, A_4	$32\ cm^2$
a_1, a_3	$0.071\ cm^2\sqrt{cm^3/gr}$
a_2, a_4	$0.057\ cm^2\sqrt{cm^3/gr}$

Using the control laws (16) and (17) with noisy measurements, with normal distribution and amplitude $n = 0.1\ cm$, of the bottom tanks pressures, the simulation scenarios involve abrupt faults in the system. To show the robustness of the control laws, the used parameters are -10% and +10% for those related with *Tank1* and *Tank2* respectively. For illustration purposes the simulations show tanks levels instead of tanks pressures.

The first simulation scenario, *Scenario_1*, consists of a minimum phase configuration with valves positions in $\gamma_{1r} = 0.3$ and $\gamma_{2r} = 0.2$. This are rated values used to parameterize the control laws. In this scenario two sequential faults occurred: at time $T = 2000s$ the value of the cross section area of outlet hole of *Tank2* is increased by 50% (forcing the same increment in a_2); and at time $T = 5000s$ the value of the valve position changes to $\gamma_1 = 0.6$.

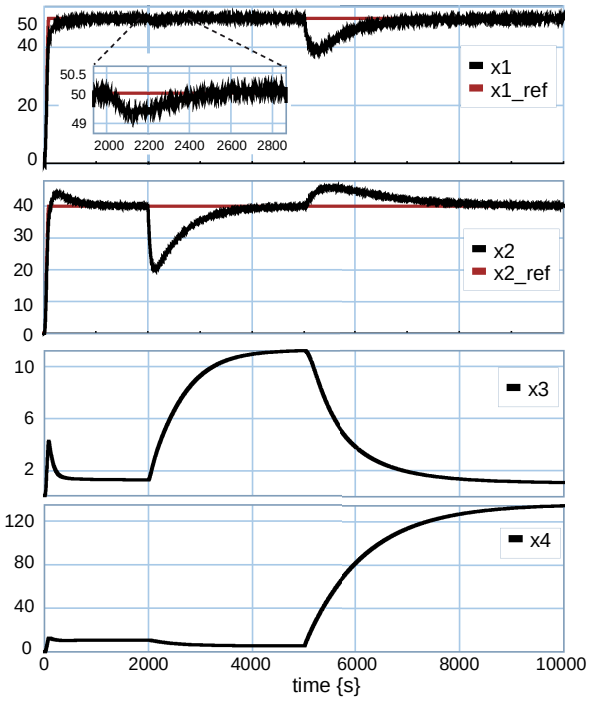

Figure 21: Tanks levels responses for sequential faults in *Scenario_1*.

The simulation responses for *Scenario_1* are shown in Figure 21 and Figure 22, which show that despite the faults occurrence the control system behaves as expected and the bottom tanks levels follow their references. For both cases, the control inputs, u_1 and u_2, force to zero the residual signals in order to reject the faults.

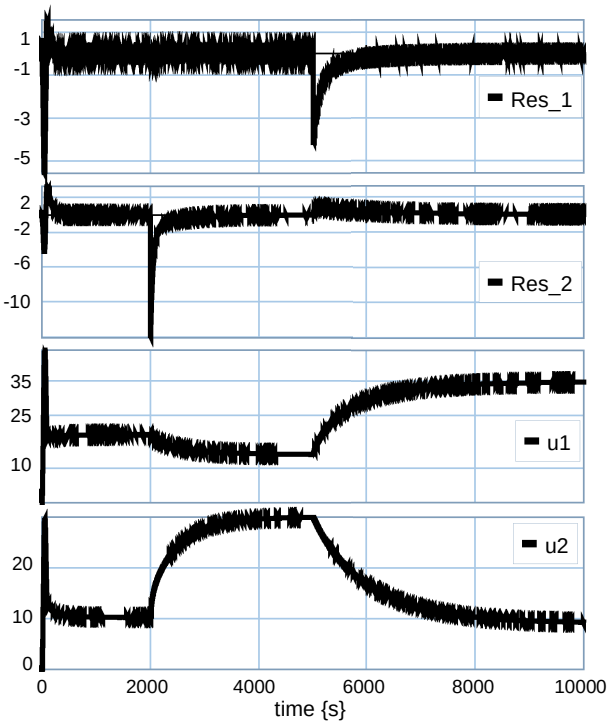

Figure 22: Residual signals and control inputs for sequential faults in simulation *Scenario_1*.

In simulation *Scenario_2* a non-minimum phase configuration is tested, where the valves position are placed at: $\gamma_{1r} = 0.7$, $\gamma_{2r} = 0.7$. Again two sequential faults occurred, the first, at time $T = 6000s$ where the value of the position valve changes to $\gamma_2 = 1$ which physically implies that *pump_2* injects all its flow to *Tank_3*; and the second, at time $T = 15000s$, where the value of the cross section area of outlet hole of *Tank1* (a_1) is increased by 50%.

In this scenario the bottom tank levels follow their references rejecting the disturbances originated by the faults occurrence as it is shown in

Figure 23. Figure 24 shows the associated residual signals and the control inputs. Here again, the control inputs force the residual signals to remain at zero to reject the faults.

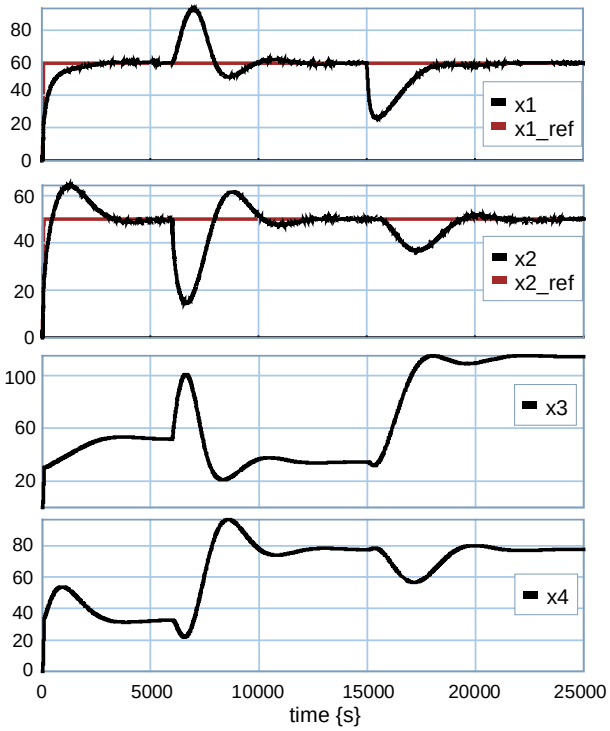

Figure 23: Tanks levels responses for sequential faults in *Scenario_2*.

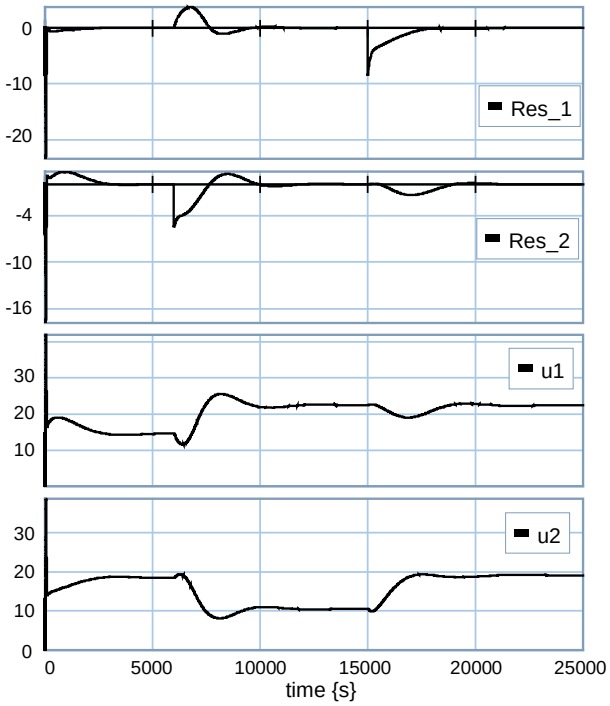

Figure 24: Residual signals and control inputs for sequential faults in simulation *Scenario_2*.

6. CONCLUSIONS

This work addressed the design of a robust controller for a multivariable four-tank system in three stages. A (partial) energy shaping and damping assignment control system design technique in the bond graph domain was first applied to obtain an almost-exact I/O-feedback linearizing controller for a simpler two-tank problem. The controller is just almost-exact because a feedback term was ignored in the (otherwise exact) control law in order to spare a measurement. The second stage proceeded to robustify the previous controller to which aim a closed-loop diagnostic bond graph was introduced. Finally, a causal manipulation was performed on the BG of the quadruple-tank that permitted handling the associated multivariable problem as two monovariable decoupled problems, each for a simple two-tank system.
Simulation results demonstrate the good response and the fault tolerance of the control system.

ACKNOWLEDGMENTS

The authors wish to thank SeCyT-UNR (the Secretary for Science and Technology of the National University of Rosario) for their financial support.

APPENDIX A: RESIDUAL SINKS

The residual sink component injects the necessary effort or flow in order to make vanish the power conjugated variable into the sink.

A residual sink element can be interpreted as an energy store where it parameter tend to zero. For example, an effort residual sink can be interpreted a C element in integral causality:

$$C\dot{e} = \Delta f$$

If the parameter C tends to zero, then $\dot{e}$ is determined by the algebraic equation $\Delta f = 0$.

Figure 25 shows the graphical representation of the effort and flow residual sink used in (Borutzky 2009).

Figure 25:flow and effort residual sink.

APPENDIX B: DIAGNOSTIC BOND GRAPH

The Diagnostic Bond Graph was first presented by (Samantaray, et al. 2006) for numerical evaluation of analytical redundancy relationships (ARR). The ARRs are calculated to perform FDI in an AFTC frame.

Basically, the DBG is obtained from a BG model of the plant injecting the plant measurements and inputs through modulated sources. The residual signal is obtained by measuring the power co-variables of the modulated sources, see Figure 26.

Reading directly from the BG the residuals are:

$$\begin{aligned} res1 &= C_1\dot{x}_1 + a_1\sqrt{x_1} + a_2\sqrt{x_2} - (1-\gamma)u \\ res2 &= C_2\dot{x}_2 + a_2\sqrt{x_2} - \gamma u \end{aligned} \qquad (18)$$

As can be noted in (18), the residuals depend on system parameters. If the model represents perfectly the controlled system, then the residual signals are zero. The differential causality is an advantage in FDI, because no initial states are necessary to evaluate the residuals.

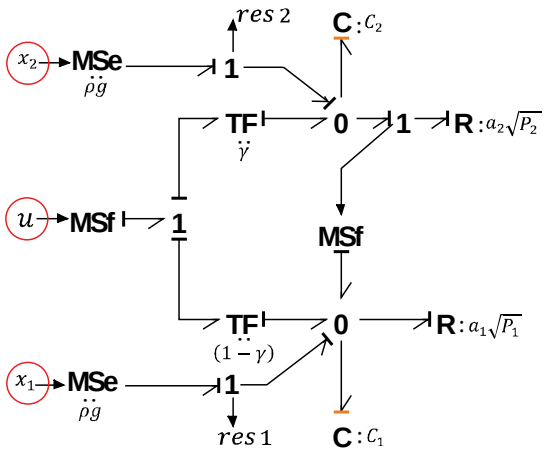

Figure 26: Diagnostic Bond Graph of the two tank system. Plant measurements to be fed into the DBG encircled in red.

REFERENCES

Abdullah A., Zribi M., "*Control Schemes for a Quadruple Tank Process*". International Journal of Computers communications and control, ISSN 1841-9836, Volume:7(4):594-604, 2012.

Blanke, M., Kinnaert, M., Lunze, J., Staroswiecki, M. "Diagnosis and Fault-Tolerant Control". Second Edition, Springer-Verlag.. 2006.

Borutzky, W. "*Bond graph model-based fault detection using residual sinks*". Proceedings of the Institution of Mechanical Engineers, Part I: *Journal of Systems and Control Engineering*, Volume 223, 2009, pp. 337-352.

Isermann, R. "*Fault-Diagnosis Systems*" Springer-Verlag. 2006.

Junco, S. *"Lyapunov Second Method and Feedback Stabilization Directly on Bond Graphs"*. Proc. ICBGM'2001, SCS-Simulation Series, 33:1, pp. 137-142.

Junco, S. "*Virtual Prototyping of Bond Graphs Models for Controller Synthesis through Energy and Power Shaping*". Conference on Integrated Modeling and Analysis in Applied Control and Automation (IMAACA 2004).

Johansson, K. "*The Quadruple-Tank Process A multivariable laboratory process with an adjustable zero*". IEEE Transactions on Control Systems Technology, 2000.

Johnsen, Jøgen and Allgöwer, Frank. "*Interconnection and Damping Assignment Passivity-Based Control of a Four-Tank System*". Lecture Notes in Control and Information Sciences. Lagrangian and Hamiltonian Methods for Nonlinear Control 2006. Springer Berlin Heidelberg publisher. Vol. 366.2007, pages 111-122.

Limon, D. Alvarado, I. Alamo, T. Camacho, E.F. "*Robust tube-based MPC for tracking of constrained linear systems with additive disturbances.*"Journal of Process Control. . Vol 20.Nro 3. 2010. pages 248-260.

Nacusse, M. Junco, S. "*Passive Fault tolerant control: A bond graph approach*". Conference on Integrated Modeling and Analysis in Applied Control and Automation (IMAACA 2011).

Ortega, R. Van der Schaft, A., Castaños, F., Astolfi, A. "*Control by Interconnection and Standard Passivity-Based Control of Port-Hamiltonian Systems*". IEEE Transactions on Automatic Control, Vol. 53, No. 11. (December 2008), pp. 2527-2542,doi:10.1109/TAC.2008.2006930.

Ortega, R., Van der Schaft, A., Maschke, B., Escobar, G. "Interconnection and damping assignment passivity-based control of port-controlled Hamiltonian systems". Automatica, Volume 38, Issue 4, April 2002, Pages 585-596.

Samantaray, A. Medjaherb, K. Ould Bouamama, B. Staroswieckic, M. Dauphin-Tanguy, G. "*Diagnostic bond graphs for online fault detection and isolation*". Simulation Modelling Practice and Theory Volume 14, Issue 3, April 2006, pages 237-262.

Sontag, E. "*Mathematical Control Theory: Deterministic Finite Dimensional Systems*". Second Edition, Springer, New York, 1998.

Zhang, Y. Jiang. J. "*Bibliographical review on reconfigurable fault-tolerant control systems*" Annual Reviews in Control, Vol. 32, No. 2. (December 2008), pages 229-252.